



Contents list available at IJRED website

Int. Journal of Renewable Energy Development (IJRED)

Journal homepage: <http://ejournal.undip.ac.id/index.php/ijred>



Research Article

Thermal Performance Comparison of Parabolic Trough Collector (PTC) Using Various Nanofluids

Ashutosh Shirole^{a*}, Mahesh Wagh^a, Vivek Kulkarni^b

^aDepartment of Technology, Shivaji University, District Kolhapur, Maharashtra, India

^bSanjay Ghodawat Group of Institutions, Faculty of engineering, Atigre, District Kolhapur, Maharashtra, India

ABSTRACT. The objective of this paper is to investigate the theoretical performance of Parabolic Trough Collector (PTC) using various nanofluids. The theoretical performances are calculated for Al₂O₃, graphite, magnetite, SWCNH, CuO, SiO₂, MWCNT, TiO₂, Fe₂O₃, and ZnO in water nanofluids. The heat transfer equations, thermodynamic properties of nanofluid and pumping power are utilised for the development of novel thermal model. The theoretical thermal efficiency of the PTC is calculated, and the economic viability of the technology is predicted for a range of nanofluid concentration. The results showed that the thermal conductivity increases with the concentration of nanoparticles in the base fluid. Magnetite nanofluid showed the highest thermal efficiency, followed by CuO, MWCNT, ZnO, SWCNH, TiO₂, Fe₂O₃, Al₂O₃, graphite, and SiO₂, respectively. The study reveals that MWCNT at 0.4% concentration is the best-suited nanofluid considering thermal gain and pumping power. Most of the nanofluids achieved optimum efficiency at 0.4% concentration. The influence of mass flow rate on thermal efficiency is evaluated. When the mass flow rate increased from 70 Kg/hr to 90Kg/hr, a 10%-20% efficiency increase is observed. Dispersing nanofluids reduces the levelized cost of energy of large-scale power plants. These findings add to the knowledge of the scientific community aimed explicitly at solar thermal energy technology. The report can also be used as a base to pursue solar thermal projects on an economic basis.

Keywords: PTC thermal performance, heat transfer, PTC performance, Nanofluids, levelized cost of PTC, modelling of PTC, pumping power.

Article History: Received: 28th Oct 2020; Revised: 12th June 2021 ; Accepted: 27th June 2021; Available online: 18th July 2021;

How to Cite This Article: Shirole A, Wagh, M, Kulkarni V. (2021) Thermal Performance Comparison of Parabolic Trough Collector (PTC) Using Various Nanofluids. *Int. Journal of Renewable Energy Development*, 10(4), 875-889
<https://doi.org/10.14710/ijred.2021.33801>

1. Introduction

Globally, 80% of consumed energy comes from fossil fuels (MNRE-UNIDO 2017). However, fossil fuel use has resulted in harmful effects on the environment. Therefore reliance on fossil fuels is being reduced by using renewable energy. Superabundant and free availability of solar energy makes it a popular choice (Biswakarma *et al.*, 2020). Also, it can be utilised as both high grade and low-grade energy. So more research is focused on solar energy. Applications of Solar energy technology are classified into solar thermal and photovoltaic. However, solar thermal had a lousy run since the last decade and is losing against solar photovoltaic. The reason behind this is the price of electricity generated from photovoltaic solar cells has abated exponentially. However, solar thermal can produce quality and stable power. To make solar thermal systems cost-competitive, the efficiency of solar collectors must be improved. In this direction, much research is focused on thermal performance improvement in solar concentrating collectors.

The conventional heat transport fluid (HTF) used in solar collectors are subjected to poor thermal and absorption properties. These fluids have low heat carrying capacity, which puts a limit on maximum achievable

thermal efficiency. It is observed from previous literature that dispersing metallic or non-metallic solid particles in base fluids can break those limits. In the initial stages, micrometre or millimetre solid particles were used, but this led to significant problems like rapid settling of solid particles in fluids and high-pressure drop, which questioned their practical application viability. However, the discovery of nanofluid boosted this concept. Nanofluids are associated with a family of nanotechnology-based HTF composed of conventional heat transfer fluids with nanosized particles dispersed in them to improve their thermal stability. Improved thermal stability is a result of increased surface area, heat capacity, heat transfer rate and high convective heat transfer coefficient. The dispersion of nanofluids also ensures uniform temperature along the receiver's length, which reduces the temperature gradient and drives high thermal performance (Shanthi *et al.*, 2012). Among all solar thermal collectors and technologies, parabolic trough collector (PTC) has shown the most remarkable progress. This can be owed to substantial experience linked with systems. Also, consistent efforts made to establish and nurture small scale manufacturing business as well as micro-enterprises to fabricate and distribute these systems have played a pivotal role in commercializing PTC technology. PTC is

*Corresponding authors: ashu11121315@gmail.com; waghmahesh2006@gmail.com; vkku20@rediffmail.com

the most mature technology, due to which it has been the first choice of investors among solar thermal technologies. Lately, various researchers have put forth the concept of nanofluid's application in solar receivers (Hajabdollahi & Hajabdollahi, 2016). Many experimental and analytical or numerical explorations have already been conducted. However, studies elaborating the application of nanofluid in PTC are not numerous. (Mohammad Zadeh *et al.*, 2015) Earlier in the year 2011, Taylor *et al.* (2011) investigated graphite nanoparticle with therminol VP-1 as a base fluid in dish collector and showed 11% improvement in efficiency. Li *et al.* (2011) experimented using Al_2O_3 , ZnO, MgO and concluded that ZnO is most suitable for nanofluid applications in solar collectors. Vajjha and Das (2012) considered a mixture of water-ethylene glycol as base fluid and dispersed Al_2O_3 , CuO, and SiO_2 nanoparticles. Al_2O_3 nanofluid at 1% concentration showed a 31.9% increase in heat transfer coefficient. However, the study is useful for colder regions only. Al-Mashat and Hassan (2013) examined experimentally Al_2O_3 water nanofluid's performance in evacuated U tube collector. They considered 0.3%, 0.6%, 1% of volume concentration which produced 0.6%, 6%, 28.4% efficiency enhancement respectively. In a subsequent study, Tyagi *et al.* (2013) examined Al_2O_3 nanofluid theoretically using the finite difference technique, which revealed that 5% - 10% higher efficiency could be achieved using PTC. Faizal *et al.* (2013) showed that the plant size of PTC could be reduced by 37% using MWCNT-water nanofluid. Waghole *et al.* (2014) experimentally investigated heat transfer network and friction factor of Ag nanofluid in a PTC with and without tape inserts. They observed a 13.5%-20.5% increase in enhancement efficiency. Nagarajan *et al.* (2014) reviewed nanofluids for solar collector applications, explaining the mechanism of every nanofluid property. They reported that the nanofluid applications are in the early stages, so very few literature pieces of theoretical investigation are available, and more research work is needed to be done.

Bajestan *et al.* (2015) analysed the heat transfer characteristic of PTC using TiO_2 nanofluid and obtained 21% maximum enhancement of the heat transfer coefficient. Sabiha *et al.* (2015) performed an experimental investigation of SWCNH water nanofluid in an evacuated tube solar collector and delineated that the highest efficiency of 94.73% at 0.25% weight. Later this year, Mwesigye *et al.* (2015a) performed simulation using ANSYS design modeller and observed that Al_2O_3 nanofluid increases thermal efficiency by 35%, 74%, 76% at 4%, 6%, and 8% concentration, respectively. Coccia *et al.* (2016) conducted an experimental study of Fe_2O_3 , TiO_2 , SiO_2 , ZnO, Al_2O_3 , Au, water-based nanofluids in PTC and concluded that only Au, TiO_2 , ZnO, Al_2O_3 show a small improvement. No significant improvement is observed compared to water. In a subsequent study, Ghasemi and Ranjbar (2016) analysed PTC with nanofluid using GAMBIT and ANSYS fluent software. They reported that the increase in heat transfer using Al_2O_3 is 28% and CuO 35%, at 0.03 concentration. Shanthi *et al.* (2017) provided a review on heat transfer escalation using nanofluids and underlined the important role played by nanoparticles in shaping heat transfer properties. Later this year, Sekhar *et al.* (2017) experimentally checked thermal efficiency improvement using Fe_2O_3 , Al_2O_3 , CeO_2 in water and obtained 23%, 25%, 27% efficiency improvement compared to the water. In a creative study, Potenza *et al.* (2017)

considered an unusual approach to analyse gas-phase nanofluid with CuO nanopowder in PTC. The study demonstrates no significant improvement in thermal efficiency. Hoseinzadeh *et al.* (2017a) experimentally investigated Al_2O_3 /Water and SiC/water nanofluid's application in a two-phase closed thermosiphon system. They observed that 2% Al_2O_3 /Water shows a 10% increase in thermal efficiency, whereas SiC/water nanofluid having 2% concentration performs 1.11 times better than pure water. Genc *et al.* (2017) administered a numerical study employing Al_2O_3 nanofluid in flat plate collectors having 1%, 2%, 3% concentration of nanoparticles and reported the highest thermal efficiency of 83% at 0.06 kg/sec mass flow rate for 1% concentration. In the following year, Kasaiean (2018) used MATLAB code to evaluate MWCNT/water nanofluid's effectiveness in PTC and observed a 15% increment in the convective heat transfer coefficient. Siavashi *et al.* (2018) studied SWCNH/water nanofluid utilizing MRTLBM code. The particular solar collector employed in the study was of huge interest. He employed direct absorption-type solar receiver. The study stated that nanoparticle addition increases solar absorption, and hence thermal efficiency is improved substantially. On the contrary, increasing the concentration above a specific limit will result in negative performance. Ozsoy and Corumlu (2018) carried out experimental trials on thermosiphon evacuated tube solar collector. They investigated efficacy of Ag/ H_2O nanofluid as HTF and achieved 20.7%–40% efficiency improvement in thermal efficiency. Kolekar and Patil (2018) analysed the thermal performance of PTC working with Al_2O_3 water nanofluid having 0.5% concentration. They reported a ten percent improvement in thermal efficiency.

Krishna *et al.* (2018) conducted numerical trials to find better nanofluid for heat transfer in solar flat plate collector. They used ANSYS fluent software and stated that CuO shows higher efficiency than Al_2O_3 . Later in the same year, Kang *et al.* (2018) reported that CuO/water HTF having 40 nanometers has 2% high efficiency than nanoparticle having 80 nanometers. Subramani *et al.* (2018) conducted an experimental exploration using TiO_2 deionised water as nanofluid in PTC. They reported 8.66% thermal efficiency enhancement at 0.2% volume concentration. In the following year, H. Fathabadi (2019) carried out a theoretical and experimental study to evaluate thermal performance PTC using CuO- H_2O Nanofluids for 0.5%-3.5% concentration range. They concluded that adding CuO nanoparticles up to 1.5% increases efficiency by 11%. Hoseinzadeh *et al.* (2019b), again in 2019, numerically investigated pulsating laminar and turbulent Al_2O_3 /Water nanofluid flow as HTF on different flow regimes. The results showed that higher thermal efficiency could be achieved with Al_2O_3 /Water relative to water alone; however, it also causes a significant pressure drop across pipe in both turbulent (3000 Reynold no) and laminar (100-2000 Reynold number). In the subsequent study, Hoseinzadeh *et al.* (2019c) numerically explored pulsating Al_2O_3 /Water nanofluid in three different cross channels and made a remarkable observation that increasing volume concentration decreases outlet fluid temperature. They added that nanoparticles lower the heat capacity of fluid, whereas nanoparticles increase heat absorption potential, resulting in increased heat flux.

The literature reveals that Al_2O_3 , graphite, magnetite (Fe_3O_4), SWCNH, CuO, SiO_2 , MWCNT, TiO_2 ,

Fe₂O₃, and ZnO nanofluids are cited extensively for efficiency improvement in PTC. The aforementioned nanofluids have shown considerable improvements and hence are a potential choice as HTF in PTC. Each nanofluid exhibits different thermodynamic behaviour, which impacts PTC performance differently. Studies published before have considered single to three nanofluids with a limited concentration range. Therefore it becomes indeed necessary to have a comparison of a maximum number of nanofluids. Many researchers have not touched the cost-benefit analysis of PTC using nanofluids. So it can also be incorporated. The primary objective of the paper lies in comparing a range of nanofluids for a wide concentration range. The second objective is to identify the best possible nanofluids for PTC application among all potential choices and calculate their optimum concentration satisfying technical and economic feasibility. In this paper, an effort has been made to compute the theoretical performance of PTC using Al₂O₃, graphite, magnetite, SWCNH, CuO, SiO₂, MWCNT, TiO₂, Fe₂O₃, and ZnO. A theoretical model is tried to develop using all aforementioned nanofluids to find the influence of nanofluid parameters on heat transfer grid of PTC for a wide range of concentration. The study also addresses the economic viability of PTC technology to attract significant investment in various business models for power generation using PTC.

2. Methodology

This section covers methodology adopted for the study. It also describes energy equilibrium in PTC and mathematics behind heat transfer framework in PTC. The Fig 1a represents working of PTC. The Fig 1b shows methodology adopted for study. The process starts with determining input parameters. This includes dimensions of PTC, solar irradiance and concentration range of nanofluids. Next nanofluid properties are calculated. Then

heat transfer analysis, thermal modelling is done and pumping power is calculated. Finally economic viability of nanofluids application is checked using LCOE and Tpb.

2.1 Nanofluid properties

The section describes thermophysical properties nanofluids. These properties are thermal conductivity, density, specific heat and dynamic viscosity of nanofluids. According to Sivashi *et al.* (Siavashi *et al.*, 2018), the Hamilton crosser model shows a close agreement with experimental data for thermal conductivity of nanofluid.

$$k_{nf} = k_{bf} \left[\frac{k_{np} + (n-1)k_{bf} + (n-1)(k_{np}-k_{bf})\phi}{k_{np} + (n-1)k_{bf} - (n-1)(k_{np}-k_{bf})\phi} \right] \quad (1)$$

'n' is a shape factor that is 2 for spherical nanoparticles, and ϕ is the concentration of nanoparticles in water, k_{bf} , k_{np} k_{nf} is the thermal conductivity of the base fluid, nanoparticle, nanofluid, respectively.

The density (ρ) and specific heat (Cp) are calculated as (Siavashi *et al.*, 2018),

$$\rho_{nf} = (1-\phi)\rho_{bf} + \phi\rho_{np} \quad (2)$$

$$Cp_{nf} = \frac{(1-\phi)\rho_{bf}Cp_{bf} + \phi\rho_{np}Cp_{np}}{(1-\phi)\rho_{bf} + \phi\rho_{np}} \quad (3)$$

$$\mu_{nf} = \frac{\mu_{bf}}{(1-\phi)^{2.5}} \quad (4)$$

$$\mu_{nf} = \mu_{bf}(1 + a\phi + b\phi^2) \quad (5)$$

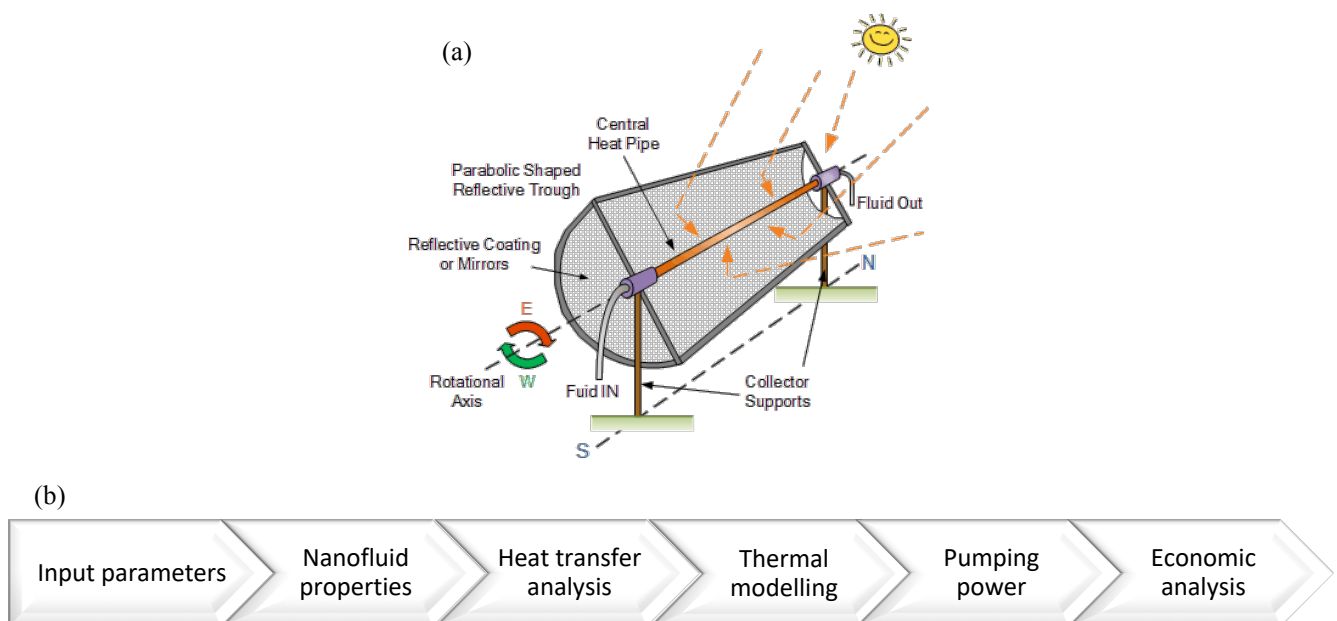


Fig 1a. Schematic diagram of PTC (Panchal. *et al.*, 2018) and (b) Methodology

Table 1
 Properties of nanoparticles

Nanoparticle	ρ (kg/m ³)	C_p (J/kgK)	k (W/mK)	Diameter (nm)
Al ₂ O ₃	3970	765	40	47
Graphite	2210	709	1950	130
Magnetite	5810	670	703	36
SWCNH	1100	750	6000	67
CuO	6500	533	17.65	30
SiO ₂	2220	745	1.38	12
MWCNT	2100	711	3000	40
TiO ₂	4175	710	8.4	21
Fe ₂ O ₃	5180	670	6.9	13.3
ZnO	5630	494	27.2	30
Water	999.1	4179	0.613	-

Table 2
 Properties of nanofluid

ϕ	ρ_{nf}	C_p	k_{nf}	μ_{nf}
0.01	1226.19	3268.55545	0.74	0.001305
0.02	1453.28	2642.64362	0.90	0.001752
0.03	1680.37	2185.90681	1.11	0.002447
0.04	1907.46	1837.92234	1.39	0.003597

With the help of Brinkman model, effective viscosity (μ) is computed using the Brinkman model, as shown in equation (4) (Brinkman, 1952). In order to simulate the results under similar circumstances (Bellos & Tzivanidis, 2018c), general equation (4) is chosen. However, equation (4) shows anomalous results for CNT nanofluids. Hence for these fluids, Fedele (Bobbo *et al.*, 2012) proposed equation (5). It should be noted that the selected model in equation (1), (4), (5) are general models and do not consider nanoparticle diameter and fluid temperature. Nanofluid's thermal conductivity's enhancement and nanoparticle diameter are directly correlated (Sundar *et al.*, 2017a); however, this assessment remains out of scope. The equation particularly considers fluid properties only, but these limitations are shared among all the analyzed nanofluids and yield good result.

2.2 Material properties

Analyzing nanofluids' properties is highly relevant since they determine the magnitude of the collector's performance enhancement. Previous literature studies showed that the HTF's thermal properties enhance with nanoparticle concentration (Sandeep and Arunachala, 2017). However, when the optimum value of concentration in any base fluid is crossed, sedimentation and aggregation phenomenon is observed, which reduces collector performance. This indicates the non-uniform dispersion of nanoparticles in a fluid. Besides, a very high

concentration of nanoparticle affects density and viscosity inversely. The density and viscosity cause a significant pressure drop across the pipe, leading to high pumping power to circulate fluid or maintain fluid flow, which is undesirable. The properties of the base fluid and nanoparticles are shown in Table 1. (Hatami and Jing, 2017), (Gorji and Ranjbar, 2016), (Siavashi *et al.*, 2018), (Kim *et al.*, 2016), (Tong, Kim and Cho, 2015), (Bellos, 2018b), (Kaya, Arslan and Eltugral, 2018).

The properties of water-based nanofluid are calculated according to equation (1), (2), (3), (4), (5) for a range of 0 to 10 % nanofluid concentration. The sample calculation of Al₂O₃ nanofluid for the range of 0 to 4% concentration is shown in Table 2. Similar to be followed to 10% concentration by each nanofluid. Fig. 2 to 5 demonstrates the thermal properties of considered nanofluids. The thermal properties like density, specific heat, thermal conductivity and dynamic viscosity are displayed in response to increasing concentration. These results are validated with Khin *et al.* (Khin *et al.*, 2017).

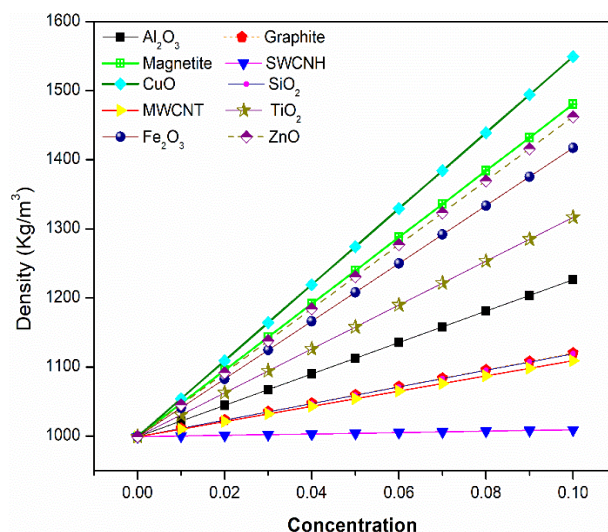


Fig 2. Effect of concentration on density

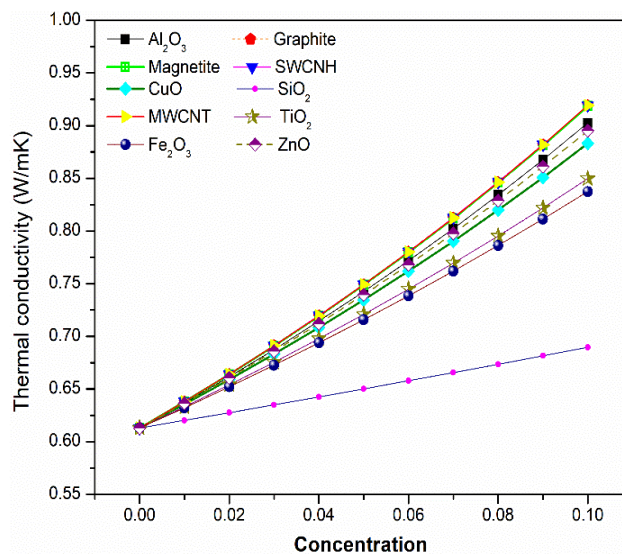


Fig 3. Effect of concentration on k

Fig. 2 exhibits the effect of nanoparticle concentration on fluid's density. It can be observed that the density of nanofluid increases significantly with an increase in concentration. CuO nanofluid is having the steepest line compared to other nanofluids, whereas SWCNH has very little influence on water density. The curve for SWCNH is nearly horizontal. The former effect is due to the massive difference in densities of the base fluid and CuO nanoparticle. Latter is owed to a small difference between densities of water and SWCNH. An increase in density results in high friction factor, causing considerable pressure drop across pipe, which is undesirable effect (Nabati Shoghl *et al.*, 2016).

Fig 3 depicts the effect of nanoparticle concentration on the fluid's thermal conductivity, which governs the heat transfer coefficient. It can be observed that all nanofluids follow a similar trend line with $\pm 0.2\%$ variation, only SiO₂ being an exception. SWCNH, MWCNT and graphite show the highest thermal conductivity enhancement of about 49.96%. It is observed that thermal conductivity increases linearly with concentration. These results are supported by (Yu *et al.*, 2011). The increased thermal conductivity of nanofluids cannot be solely attributed to high thermal conductivity of nanoparticles but also the interaction between nanoparticle and fluid (Simpson *et al.*, 2018).

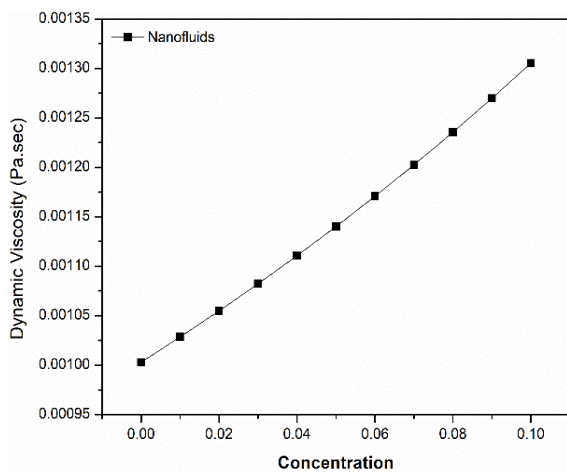


Fig 4. Effect of concentration on μ

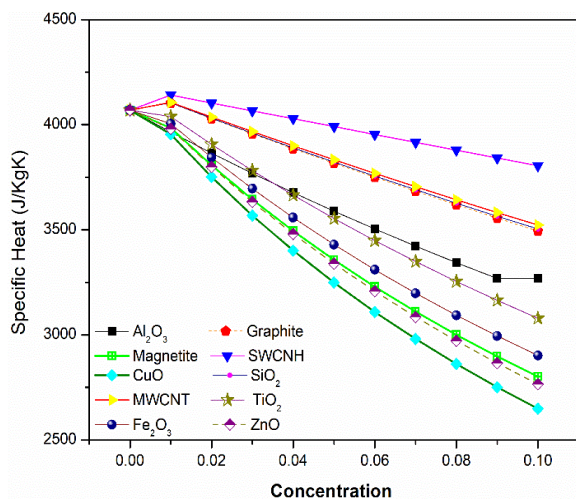


Fig 5. Effect of concentration on C_p

Thermal conductivity has heavy dominance on Nusselt number and convective heat transfer coefficient. Therefore improved thermal conductivity with concentration prognosticates high thermal performance. Fig 4 reflects the effect of nanoparticle concentration dynamic viscosity. The parabolic curve indicates an exponential increase in dynamic viscosity concerning nanoparticle concentration. Since dynamic viscosity is the only function of concentration rather than nanoparticle properties, as shown in equation (4), all nanofluids have the same viscosity for a given concentration and temperature. It is important to note that viscosity is a measure of frictional resistance between relative layers and therefore increase in same attenuates mobility of fluid (Hussein *et al.*, 2013). As discussed by Hoseinzadeh *et al.* (2017a), reduced mobility results in increased energy absorption. However, the increased friction between layers engenders high-pressure drop and pumping power consumption. Increased dynamic viscosity also leads to sedimentation and augmentation, which is highly undesirable effect. In severe condition, it may lead to pump failure, so optimum concentration must be identified to balance heat gains with pressure drop (Kim *et al.*, 2016b). However, the presence of nanoparticle leads to reduced specific heats shown by Fig 5. This lends support to previous findings in literature (Murshed, 2011). This is an adverse effect and attributed to the extensively low specific heat of nanoparticles. It is crucial to mention that thermal capacity of fluid is a function of specific heat and density. Therefore decrease in specific heat might result in decrease in heat capacity unless density improves significantly. Hence advantage of increased heat absorption due to high thermal conductivity and viscosity of nanofluid can only be utilized if fluid's heat carrying capacity is high.

2.3 Parabolic trough collector

The energy balance equation presented below indicates thermal performance, ultimately calculating the collectors' thermal efficiency under assumed conditions. Heat energy available at parabolic trough collector equals the algebraic sum of energy gained by HTF and losses occurring between receiver collector and environment.

$$Q_u = m C_p (T_o - T_i) \tag{6}$$

When HTF of specific heat (C_p) flowing at a constant mass flow rate (m) enters the receiver with temperature T_i , it absorbs heat energy, due to which its temperature rises continuously termed as T_o . Then useful heat gain (Q_u) can be calculated as in equation (6). This model is strictly limited to experimental study (Mweigye and Meyer, 2017). A typical thermal performance of PTC is shown by equation (7). (Kalogeriou, 2014). This general model gives more prominence to PTC's geometry.

$$Q_u = F_R [S A_a - A_r U_l (T_i - T_{am})] \tag{7}$$

Where S is absorbed solar radiation, A_a , A_r is aperture area and receiver area, respectively, U_l is the overall heat loss coefficient; T_{am} is ambient temperature.

Heat removal factor (F_R) is calculated as in equation (8), where collector efficiency factor (F') is given in equation (9).

$$F_R = \frac{mC_p}{A_r U_l} \left[1 - \exp\left(\frac{-U_l F' A_r}{mC_p}\right) \right] \quad (8)$$

$$F' = \frac{\frac{1}{U_l}}{\frac{1}{U_l} + \frac{D_{ro}}{(h_f D_{ri})} + \left(\frac{D_{ro}}{2k}\right)} \quad (9)$$

Where D_{ro} , D_{ri} , h_f , and k represents outside, inside diameter of the receiver pipe, convective heat transfer coefficient of fluid and thermal conductivity of pipe material.

Heat gain can also be represented as a function of convective heat transfer coefficient (Bellows and Tivandis, 2017). It can be referred to as a heat transfer model.

$$Q_u = A_{ri} h_f (T_r - T_{fm}) \quad (10)$$

It is necessary to clarify that A_{ri} is the inner receiver area, T_r is the mean receiver temperature, and T_{fm} is the mean fluid temperature. A_{ri} and T_{fm} can be calculated according to equation, respectively.

$$A_{ri} = \pi D_{ri} L \quad (11)$$

$$T_{fm} = \frac{T_i + T_o}{2} \quad (12)$$

The heat transfer coefficient (h_f) is shaped by fluid's thermophysical properties and fluid flow type. It is given as;

$$h_f = \frac{Nu k}{D_{ri}} \quad (13)$$

where k is the thermal conductivity of HTF. For turbulent flow through a circular pipe, Nussult number (Nu) is computed using the Dittus -Boelter equation, which is shown in equation (14) (Bellows and Tzivanidis, 2017a)

$$Nu = 0.023(Re)^{0.8} (Pr)^{0.4} \quad (14)$$

Reynolds number (Re) can be calculated as (Hatami and Jing, 2017),

$$Re = \frac{\rho V D_{ri}}{\mu} \quad (15)$$

Prandtl number (Pr) is given as (Bellows and Tzivanidis, 2017a),

$$Pr = \frac{\mu C_p}{k} \quad (16)$$

Where ρ , μ , C_p , k are the thermophysical properties of water-based nanofluids, and V is velocity of fluid.

The energy available at the solar collector (Q_s) is given as (Kolekar, 2018).

$$Q_s = (I_b r_b + I_d r_d)(WL) \quad (17)$$

Here I_b and I_d are incident beam and diffused solar radiation, r_b and r_d are geometric factor for beam and diffused radiation, W , L is aperture and length of reflector. Therefore it is appropriate to define thermal efficiency (η) as a fraction of total heat available at the collector, which is absorbed by HTF (Bellows and Tzivanidis, 2017a).

$$\eta_{th} = \frac{Q_u}{Q_s} \quad (18)$$

Lastly, pumping power (P_p) required to circulate fluid through the receiver is computed. Pumping power requires the friction factor (f) to be determined. The friction factor is dependent on Re . Many researchers have developed a correlation for the friction factor by regression analysis and experimental studies.

For base fluid, the water Blasius equation is used (Azmi *et al.*, 2013);

$$f = 0.3164 Re^{-0.25} \quad (19)$$

Sundar *et al.* 2017 (Sundar *et al.*, 2012b) proposed correlation for nanofluid as;

$$f = 0.3164 Re^{-0.25} (1 + \phi)^{0.1517} \quad (20)$$

Using friction factor, the pressure drop is calculated (Tripathi and Bhong, 2016). The product of volumetric flow per second of HTF inside the pipe and pressure drop across the pipe can be defined as pumping power.

$$\Delta P = \frac{f L \rho V^2}{2D_{ri}} \quad (21)$$

$$P_p = \left(\frac{\pi}{4} D_{ri}^2 V \right) \Delta P \quad (22)$$

2.4 Economic analysis

The final aim of the study is to check the economic feasibility of the application of nanofluid in PTC. LCOE is the most crucial parameter used in determining the cost-effectiveness of power plants. Analysts also use the total payback period for strengthening the confidence of investors.

Kasaiean *et al.* (Kasaiean *et al.*, 2018) have put forward below mentioned equation (23) for LCOE. With slight modification as per guidelines of NREL, LCOE is evaluated (Comello, Glenk and Reichelstein, 2017).

$$LCOE = \frac{C_{rf} Z_{investment} + Z_{maintenance}}{W_{net} \times CF \times 8760} \quad (23)$$

Where $Z_{investment}$ and $Z_{maintenance}$ are capital and operation & maintenance cost per annum, respectively, W_{net} is equal to power generation, CF is equal to the capacity factor. This factor represents a fraction of total running hours throughout the year. This factor is assumed to be 29%.

The C_{rf} is capital recovery factor, which is calculated as shown in equation (24).

$$C_{rf} = \frac{i(1+i)^n}{(1+i)^n - 1} \quad (24)$$

Here i is rate of interest, and n is the presumed collector's lifetime. The solar thermal power plant comprises various equipment, which includes supportive structure

and solar collector (Dai *et al.*, 2003). Ultimate PTC trough collector has been taken into consideration as a solar collector. The cost of the components mentioned above as capital investment is given in Table 3 (Kasaiean *et al.*, 2018)(Kurup *et al.*, 2015)(Nanofluidprice Date 2/10/2020). Kasaiean *et al.* (Kasaiean *et al.*, 2018) have suggested that maintenance and operating costs can be divided into two sections as variable and one fixed cost is composed of cooperating labour and support cost of chemicals and water has been included in variable costs. In the current study, maintenance and operating cost are estimated to be 8% of capital cost. Furthermore, the time of return on investment is represented by payback time, which is designated as in equation (25) (Kasaiean *et al.*, 2018).

$$T_{pb} = \frac{Z_{investment}}{W_{net} Coe} \quad (25)$$

Coe is the cost of energy, estimated to be 4 INR/W-hr as per the latest report.

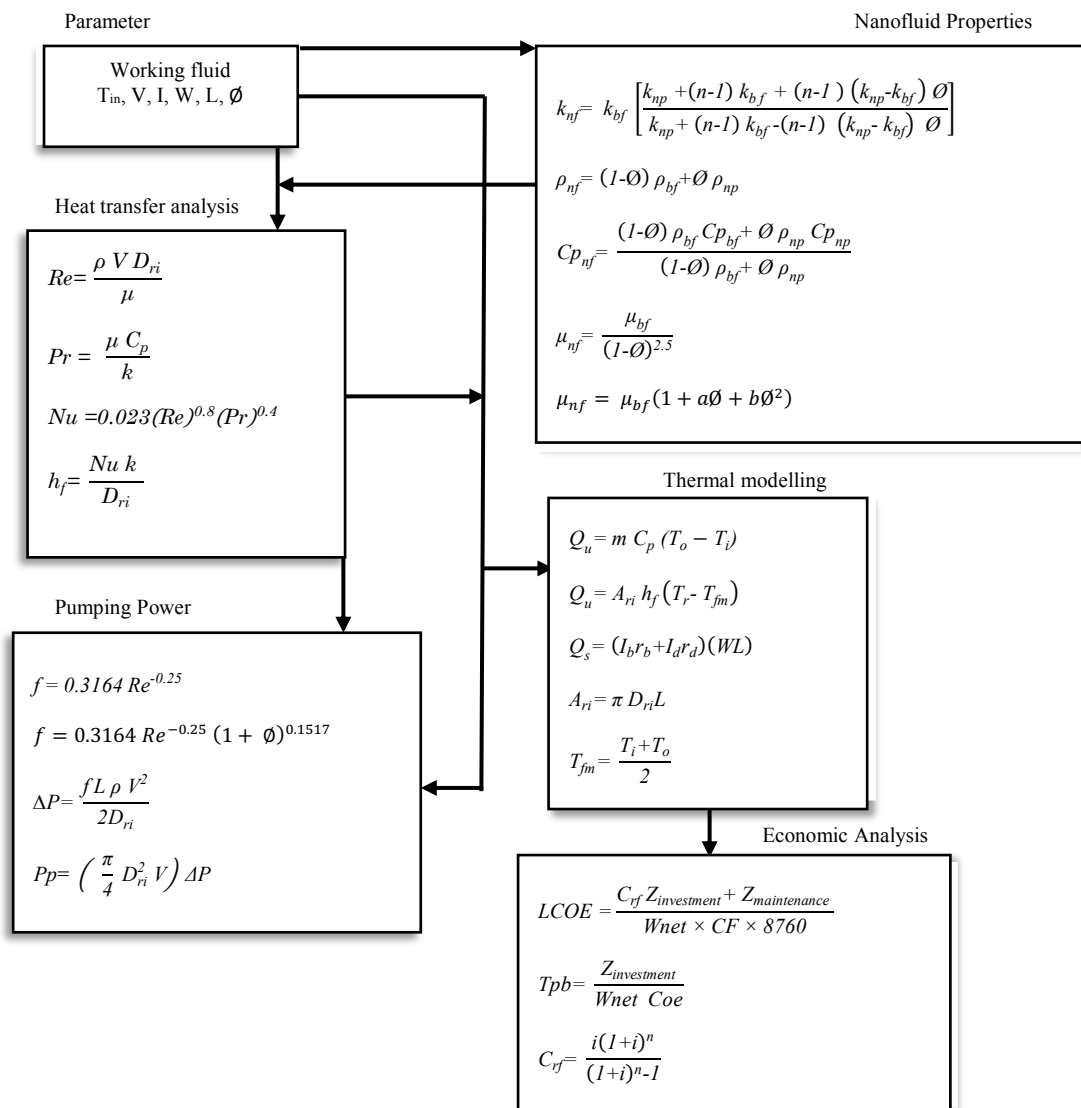


Fig 6. Methodology of model developed

2.5 Model selection

The fundamental dimensions of the solar collector chosen for study are shown in Table 4. It is essential to state that the parameters presented in Table 4 are kept constant throughout the study. The methodology adopted for the study is shown in Fig 6. The first step of study is to calculate nanofluid properties for varying range of concentration. The thermophysical properties of nanofluid are thoroughly analyzed. The next part is heat transfer analysis. This part is important to evaluate impact of heat transfer coefficient and aforementioned dimensionless number on heat transfer behaviour of nanofluid. The third part of study is to model the selected nanofluids in PTC.

As mentioned in section 2.3, there are number of models available to evaluate PTC's performance. The experimental model presented in equation (6) is feasible only to calculate heat transfer performance for limited combinations of nanofluids. The geometric model gives more weight to improvements in the collector's geometry or optical geometry and undermines the significant role of convective heat transfer coefficient. It is noteworthy that nanofluids' use improves the absorption of incident solar radiation. As a result, the convective heat transfer coefficient (h) increases. The geometric model gives mere importance to heat transfer coefficient (h), and hence any changes in h do not show observable effect on the efficiency of PTC in the former model. However, the advantage of using the heat transfer model is that it considers h as a crucial parameter and hence indicates its effect on PTC's efficiency. In accordance with the above context heat transfer model in equation (5) is radially adopted for further calculations.

Using the information presented in Table 4, heat gain is calculated with the aid of equation (5). Further pumping power calculations and economic analysis is performed, respectively. The flow diagram for the methodology adopted is shown in Fig 6. It should be stressed that the main parameters of the considered collector, velocity of fluid flow are kept constant, and all thermophysical properties, dimensionless numbers, thermodynamic constants are calculated for varying concentration of each nanofluid. This accentuates relative comparison of considered cases which is the objective of the research (Bellos and Tzivanidis, 2017a).

Table 3
Capital Cost

Component	Cost
Solar collector	12000 INR
Storage tank	3000 INR
Al ₂ O ₃	2000 INR/15g
Graphite	100 INR/15g
Magnetite	2200 INR/15g
SWCNH	30000 INR/15g
CuO	2200 INR/15g
SiO ₂	2000 INR/15g
MWCNT	2500 INR/15g
TiO ₂	2000 INR/15g
Fe ₂ O ₃	2000 INR/15g
ZnO	2000 INR/15g

Table 4
Specifications of PTC

L (m)	D (m)	I(W/m ²)	R	W (m)
1.21	0.011	517	1	1.1

3. Results and discussion

The aim of this investigation is to analyse the performance of PTC using nanofluids. The performance of PTC is governed by various parameters like Nu, Re, Pr, heat transfer coefficient. These parameters are closely related to the thermophysical properties of HTF. Since concentration influences these properties, PTC's thermal performance has been evaluated as a function of nanofluid concentration..

3.1 Dimensionless analysis

Re, Nu, Pr regulate fluid flow inside the collector absorber. These quantities vary with HTF used. Therefore it becomes crucial to study the effect of these parameters against nanofluid concentration. Fig 7 represents the effect of nanoparticle concentration on Re. Reynold's number is derived as stated in equation (15). Here to reflect the effect of only concentration, the fluid velocity is kept constant. The results indicate that for Al₂O₃, SiO₂ and graphite nanofluids, Reynold's number decreases, whereas for Magnetite, SWCNH, CuO, MWCNT, TiO₂, Fe₂O₃, ZnO, Reynold's number increases. This phenomenon can be explained by increased density and dynamic viscosity of fluid. Increased Reynolds number shows the dominance of inertia force, whereas receding Reynolds's number shows viscous force dominance.

One of the first attempts is made to show the correlation between the Prandtl number and nanoparticle concentration. Fig 8 illustrates the Prandtl number as a function of concentration. It is clear from the figure that the Prandtl number is inversely proportional to concentration except for SiO₂, which shows approximately no change. The graph is steepest in the negative direction for MWCNT, followed by CuO, SWCNH, magnetite, ZnO, Fe₂O₃, TiO₂, graphite and Al₂O₃.

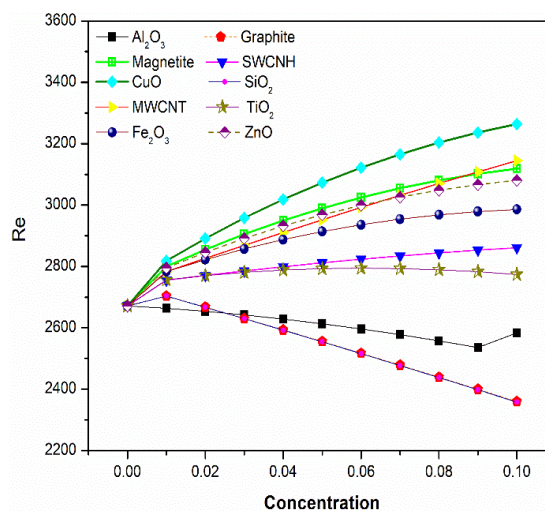


Fig 7. Effect of concentration on Re

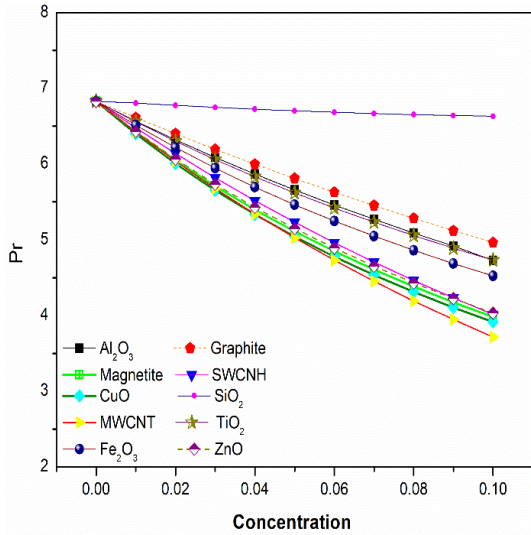


Fig 8. Effect of concentration on Pr

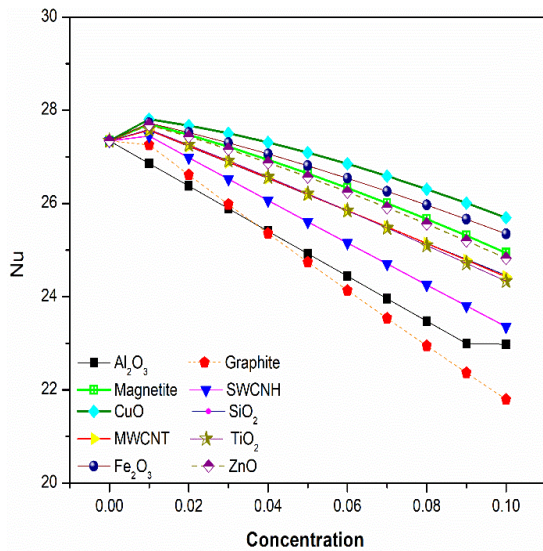


Fig 9. Effect of concentration on Nu

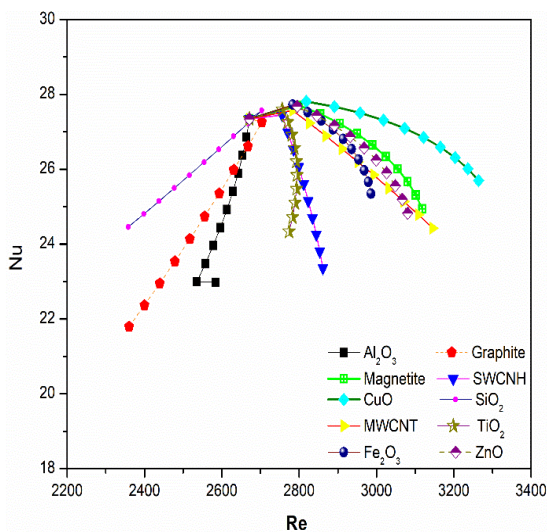


Fig 10. Effect of Re on Nu

Reduced Prandtl number is the combined effect of progressively lower specific heat, reduced mobility and elevated thermal conductivity. The significant lower Prandtl number shows that heat transfer is more likely to happen by thermal diffusion than molecular motion (Smith *et al.*, 2013). The anomalous behavior of SiO₂ is due to a low increase in thermal conductivity compared to specific heat.

Fig 9 illustrates the effect of nanoparticle concentration on Nu. It proclaims that as nanofluid concentration rises, Nusselt number decreases (Sadaghiani, Yildiz and Koşar, 2016), which does not support previous research in this area. Mwesigye *et al.* (Mwesigye, Huan and Meyer, 2015a), Sundar *et al.* (Sundar, Singh and Sousa, 2014c) have argued that Nusselt number is directly proportional to concentration. However, their calculations are only limited to cases of low concentration. Nu is the ratio of heat convected to a fluid to the thermal energy conducted within the fluid. Thus the above results are supported by the high thermal conductivity of nanofluid.

Fig 10 exhibits the relationship between Re and Nu. Re is plotted on abscissa and Nu on ordinate axis. The figure proves that Re has no general relation with Nu and is a fluid dependent phenomenon only. For Al₂O₃, graphite, SiO₂ Re is directly proportional to Nu, whereas, for rest of the considered nanofluids, Re is inversely proportional to Nu. Therefore based on results, no concrete evidence can be obtained to form general relation between Re and Nu for all nanofluids. However, it can be argued that the nusselt number is a function of both Reynolds number and Prandtl number, so above result underline important role played by Prandtl number.

Fig 11 reveals a relation between Pr and Nu. Since Nu is a function of Re and Pr and Re is a fluid dependent phenomenon; it becomes important to project relation between Pr and Nu. It can be observed that Nu is directly proportional to Pr. This is due to the high thermal diffusivity of nanofluid. Since thermal diffusivity and thermal conductivity are closely related, Pr is directly proportional to Nu. This demonstrates how crucial the Pr number is in nanofluid thermal performance assessment (Zhang, 2016).

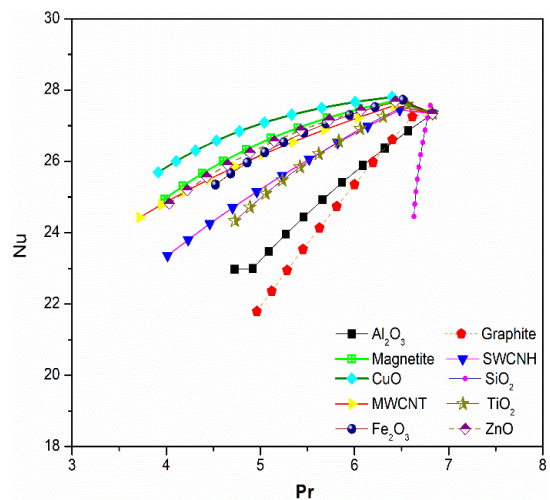


Fig 11. Effect of Pr on Nu

3.2 Heat transfer coefficient

Recently published studies have demonstrated the predominance of Re on h . Therefore it is of prime interest to identify significant parameters that govern the heat transfer network. To investigate the relative impact of Pr , Re , and h as a function of concentration, Fig 12 and Fig 13 is plotted. The Figure 12 shows a group of nanofluids of which Re increases with concentration. Figure 13 represents the findings of Al_2O_3 nanofluid, which represents the nanofluids group, of which Re decreases with concentration. Fig 12 reveals that Re continuously increases with nanoparticle concentration. Pr decreases continuously, and h increases. Fig 13 surmises that Re decreases with nanoparticle concentration. Pr decreases, and h increases simultaneously. This reveals that enhancement of h is independent of the trend in Re , and h is firmly a function of Pr . It is evident that to achieve a high value of h , low Pr is desired. Prandtl number is a relative measure of thermal boundary layer. Therefore decreasing Pr indicates thinning of thermal boundary layer, thereby increasing dT/dx (Temperature gradient). This leads to increased heat transfer. Since heat gain is a product of h and dT (Temperature difference), here, the effect of dT is absorbed in h . Hence the study questions the significance of Re and casts a new light on the dominance of Pr on heat transfer behaviour of nanofluid.

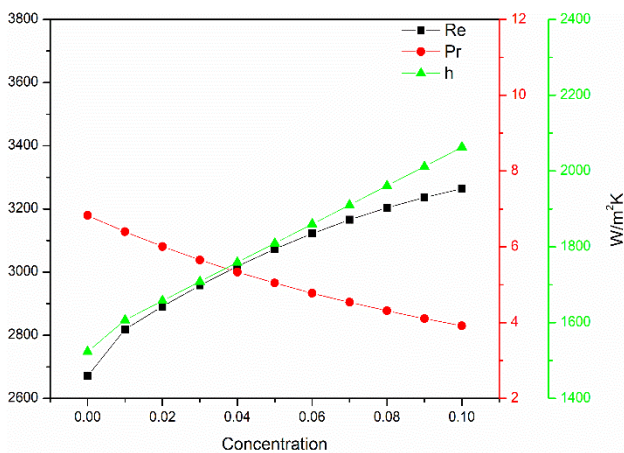


Fig 12. The relative effect of ϕ on Re , Pr , h

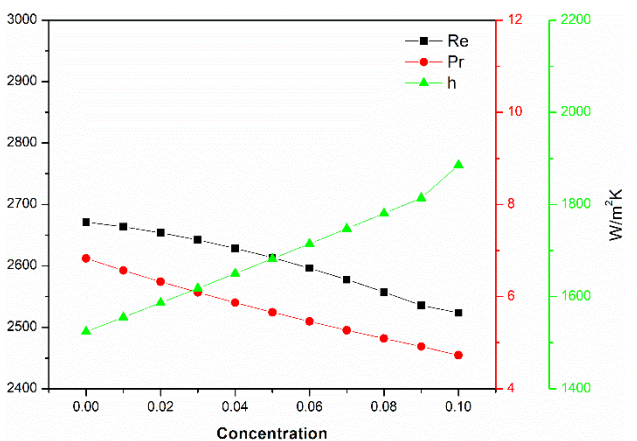


Fig 13. The relative effect of ϕ on Re , Pr , h

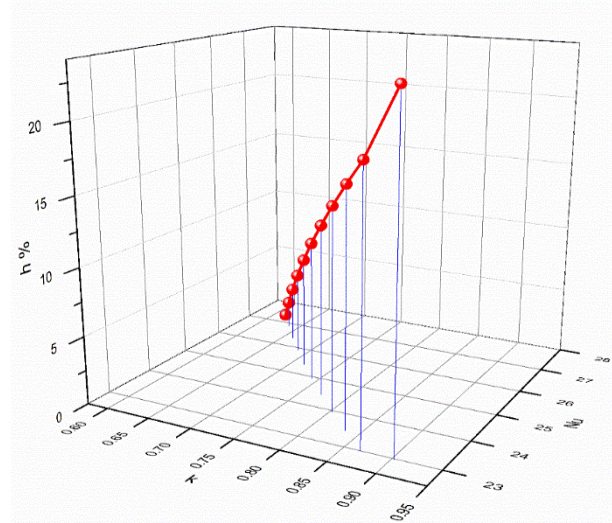


Fig 14. h as a function of Nu and k

Equation (13) states that Nu , k constrain the heat transfer coefficient. Therefore Fig 14 is plotted as a combined function of Nu and k . The graph is plotted for Al_2O_3 nanofluid only; since all nanofluids follow a similar pattern with a small variation. Fig 14 illustrates that h increases when Nu decreases and thermal conductivity increases. This result is owed to a significant improvement in k relative to declination in Nu . At 10% concentration 0.9193 W/mK of k , h attains a maximum value of 2082 W/m²K.

3.3 Thermal performance

Thermal efficiency is derived from equation (18), where $(T_r - T_{fm})$ is kept constant, and η_{th} is derived for altering values of h_f . This technique provides commensurate significance to the effect of altering h_f on efficiency. Fig 15 displays the relation between ϕ and η_{th} for concerned nanofluids. Fig 15 infers that Magnetite achieves maximum thermal efficiency enhancement followed by CuO , $MWCNT$, ZnO , $SWCNH$, TiO_2 , Fe_2O_3 , Al_2O_3 , graphite and SiO_2 . To check the model's validation, the results are correlated with empirical findings of Kolekar and Patil (Kolekar, 2018). Investigation's output shows good agreement for Al_2O_3 nanofluid. The figure shows that the thermal efficacy of PTC using nanofluid increases with nanofluid concentration linearly. It can be observed that the efficiency of SiO_2 nanofluid is highest at 1% concentration. Increasing concentration beyond 1% decreases efficiency. It must be pointed out that the efficiency of SiO_2 nanofluid is still higher compared to water, but the difference is negligible. This is owed to low thermal conductivity of SiO_2 nanofluid. At 10% concentration magnetite, CuO , $MWCNT$ shows 21%, 19%, 18% increases in efficiency, respectively. However, such high gains cannot be achieved practically since high nanofluid concentration causes a heavy pressure drop and hence requires significant pumping power.

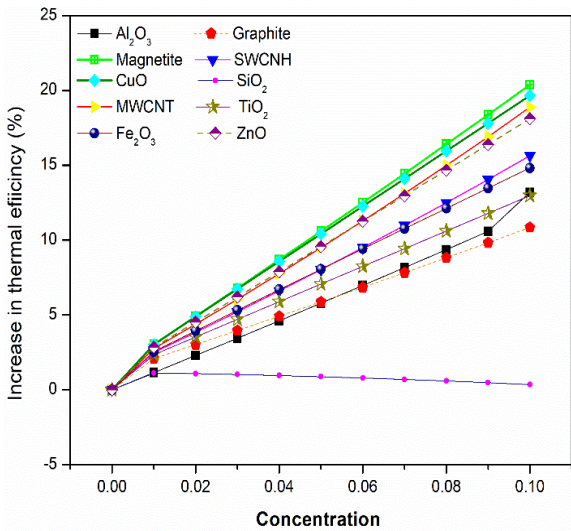


Fig 15. Thermal efficiency

Fig 16 depicts relation between HTF and mass flow rate at 0.4% concentration. To analyse the results, a particular concentration is chosen, and only mass flow rate is varied. This means all thermophysical properties are constant for a particular fluid in all three different mass rates. By doing this, the emphasis is given to highlight the mass flow rate's influence on thermal efficiency. Regarding prior knowledge, it can be concluded that increasing mass flow rate results in higher efficiency. There are two possible events behind improved thermal efficiency. One is rapid arbitrary movements of molecules and nanoparticles, causing high energy exchange between receiver and nanofluid. However, this also increases friction and hence pressure drop (Hussein *et al.*, 2013). The second one is a decrease in thermal losses occurring between HTF and tube wall of receiver. Fig 16 suggests a direct relationship between mass flow rate and thermal efficiency. When the mass flow rate increases from 70 kg/hr to 90 kg/hr instantaneous increase of 15-20 % in PTC's thermal efficiency is detected. The data connects well with Genc *et al.*(Genc, Ezan and Turgut, 2018)

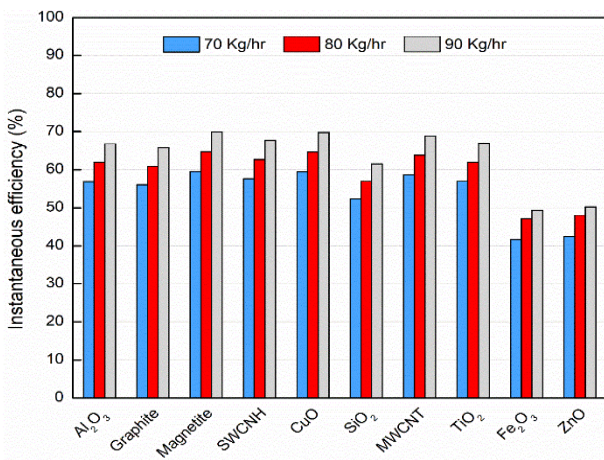


Fig.16 Effect of mass flow rate on efficiency

3.4 Pumping power

A considerable amount of power is required to circulate HTF through the collector absorber. For a constant flow rate, pumping power increases as the pressure drop across pipe increases. The pressure drop is calculated using the Darcy Weisbach equation. Pressure drop occurs due to internal friction between fluid layers and friction between fluid and absorber. In the current study, smooth pipe turbulent flow is considered, which reduces fluid friction with absorber to negligible. A high friction factor leads to a high-pressure drop and higher pumping power. A solar collector design is only acceptable if the increase in thermal efficiency outperforms the required pumping power. Hence considerable attention must be paid to the pumping power required by the system.

Fig 17 exhibits friction factor for a varying range of Re. Subramani *et al.* (Subramani *et al.*, 2017) suggested that Re is inversely proportional to friction factor. The study supports this previous finding. It can be observed that the plot is clustered between 2500 - 3000 Re. It shows that all nanofluids follow a similar pattern. The model showed a ± 2% deviation with Sundar *et al.* (Sundar *et al.*, 2017a)

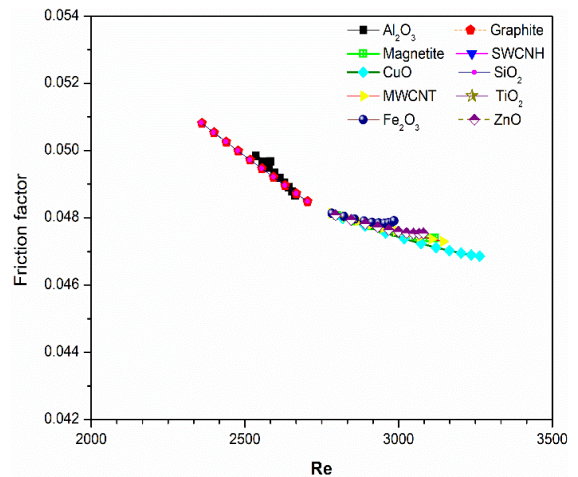


Fig 17. Friction factor

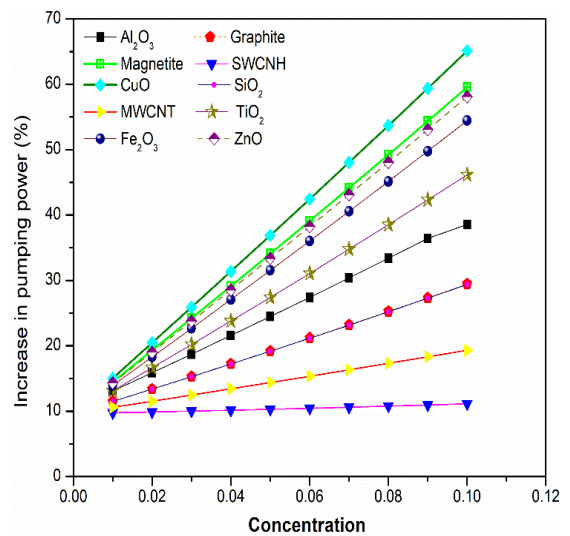


Fig 18. Pumping power consumption

Fig 18 shows an increase in percentage pumping power consumption against concentration. At 0.1% concentration, HTF only consumed 10% of the total energy produced approximately. Indeed increasing concentration resulted in high pumping power requirement. SWCNH showed the least increase in pumping power, whereas CuO depicts the highest increase in pumping power. Thus SWCNH represents the highest gain in overall efficiency.

3.5 Economic analysis

Fig 19 infers LCOE and Tpb of PTC projects using discussed nanofluids. It can be observed that graphite has lower LCOE than water. Every other nanofluid either matches or exceeds the LCOE of water by nominal value. The same results can be observed for Tpb. These results, therefore, question the economic viability of nanofluids application in PTC. This is the consequence of the high cost of nanoparticles. Nanoparticles constituted 20% in annual cost. Therefore, if the share of nanofluid's cost can be brought down by lowering the cost of nanoparticles, the technology can prove to be a game-changer in the solar thermal market. It must be emphasized that these results are derived for a very small size set-up and for a 2% concentration of nanoparticle only. Results might be different for large scale power plants since the share of nanoparticle's cost will be very low compared to the cost of power plant infrastructure.

At the end of the discussion, it can be deduced that Pr plays a crucial role in determining heat transfer characteristics. Hence more research must be done to re-examine the role played by Pr. This study has shed light on the importance of dynamic viscosity of nanofluid. Dynamic viscosity considered in the current investigation only considers the concentration of nanoparticles. Underlining the role played by dynamic viscosity, this investigation proposes further research to develop the formula for dynamic viscosity as a function of shape factor, diameter. Also, this research redraws the attention of the scientific community on the thermal conductivity of nanofluid. The incompetence between dynamic viscosity and thermal conductivity constraints heat transfer behaviour. However, the empirical results reported herein should be considered in light of some limitations.

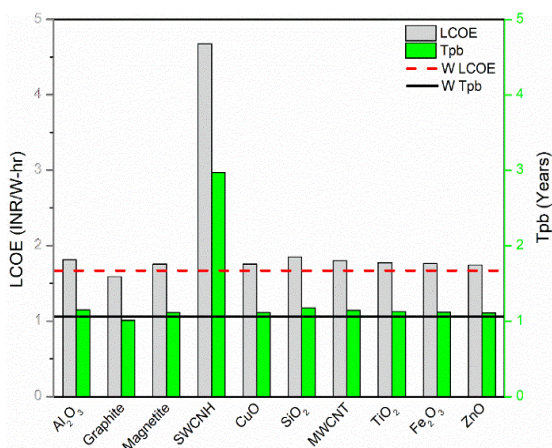


Fig 19. Economic analysis

The effect of temperature on the properties of nanofluid is ignored. Also, the losses occurring due to temperature difference between the receiver and ambient temperature are not considered. The report proclaims that high energy output can be achieved with low investment by using nanofluid, granted that the cost of nanoparticles is within a prescribed limit. Low nanoparticle's cost can further reduce LCOE. Hence further investigation is suggested in this direction.

5. Conclusion

This paper investigates the application of nanofluid in PTC. The conventional nanoparticles are selected and examined in water as a base fluid. The thermal performance of PTC using nanofluid is evaluated for a wide concentration range of 0 to 10%. The results showed that high thermal efficiency could be achieved with nanofluid due to improved heat transfer coefficient. The parametric analysis showed that thermal efficiency increases at a high flow rate. When the mass flow rate is increased from 70kg/hr to 90 kg/hr an 15 to 20% increase in instantaneous efficiency is observed. Prandtl number and thermal conductivity of nanofluid influences heat transfer behaviour of nanofluids rather than Reynold's number. Hence, more research must be done to investigate the crucial role played by the Prandtl number.

At 10% concentration, Magnetite, CuO, MWCNT showed a 21,20,19% increase in efficiency compared to water and pumping power increases by 59, 65, 19 % compared to water. So it can be concluded that MWCNT is the best suitable nanofluid for PTC application. The consumption through an increase in pumping power and gain in efficiency for all nanofluid is balanced at 4% concentration and therefore can be considered optimum value for further research. At 4% concentration, Al₂O₃, graphite, SWCNH, TiO₂, Fe₂O₃, and ZnO showed a 4.6 to 7.8 % increase in efficiency compared to water. The enhanced efficiency of the collector is solely attributed to the high thermal conductivity of nanofluid. SiO₂ nanofluid reported only a 0.9% increase in efficiency and a 17% increase in pumping power. It shows that pumping power consumption completely outweighs thermal gain and should no longer be considered a viable nanofluid in PTC application.

LCOE is high for small scale application (< 1 MW), and hence nanofluids should be considered for large scale power plants only (> 100 MW). The research in lowering the cost of nanofluid is crucial for commercialising nanofluid in power sector. This report is fruitful in developing different scales of PTC projects using nanofluid. This study can be used as a base for informing decisions to pursue projects on an economic basis.

Nomenclature

Symbol	
A	Area, m ²
C _{rf}	Capital recovery factor
C _{oe}	Cost of energy, INR/W-hr
C _p	Specific heat, J/KgK
D	Diameter, m
f	Friction factor

- | | | |
|----------------|---------------------------------|---|
| I | Solar irradiance | <i>Assessments</i> , 26(August), 105–115.
https://doi.org/10.1016/j.seta.2017.10.005 |
| Nu | Nusselt number | Bobbo, S., Fedele, L., Benetti, A., Colla, L., Fabrizio, M., Pagura, C., & Barison, S. (2012). Viscosity of water based SWCNH and TiO ₂ nanofluids. <i>Experimental Thermal and Fluid Science</i> , 36, 65–71.
https://doi.org/10.1016/j.expthermflusci.2011.08.004 |
| Pr | Prandtl number | Brinkman H., (1952). The Viscosity of Concentrated Suspensions and Solutions, <i>Journal of chemical and physics</i> . 20(4), 571–571. https://doi.org/10.1063/1.1700493 . |
| ΔP | Pressure loss, N/m ² | Coccia G., Di G., Colla L., Fedele L., Scattolini M., (2016). Adoption of nanofluids in low-enthalpy parabolic trough solar collectors : Numerical simulation of the yearly yield, <i>Energy Conversion and Management</i> . 118 306–319. https://doi.org/10.1016/j.enconman.2016.04.013 . |
| Pp | Pumping power, W | Comello S., Glenk G., Reichelstein S. (2017). Levelized Cost of Electricity Calculator : A User Guide, <i>Stanford Graduate School of Business</i> . |
| Q _u | Heat gain, W | Dai, Y. ., Huang, H. ., & Wang, R. . (2003). Case study of solar chimney power plants in Northwestern regions of China. <i>Renewable Energy</i> , 28(8), 1295–1304. https://doi.org/10.1016/s0960-1481(02)00227-6 |
| Q _s | Heat available, W | Ebrahimi-bajestan E., Charjouei M., Niazmand H. (2016). Experimental and numerical investigation of nanofluids heat transfer characteristics for application in solar heat exchangers, <i>International Journal of Heat and Mass Transfer</i> . 92 1041–1052. https://doi.org/10.1016/j.ijheatmasstransfer.2015.08.107 . |
| r | Geometrical or tilt factor | Faizal M., Saidur R., Mekhilef S., Potential of size reduction of flat-plate solar collectors when applying MWCNT nanofluid, (2013). <i>IOP Conference Series: Earth and Environmental Science</i> . 16 012004. https://doi.org/10.1088/1755-1315/16/1/012004 . |
| Re | Reynolds number | Fathabadi H., (2019). Novel solar collector: Evaluating the impact of nanoparticles added to the collector 's working fluid , heat transfer fluid temperature and flow rate, <i>Renewable Energy</i> . https://doi.org/10.1016/j.renene.2019.10.008 . |
| T | Temperature, K | Genc, A. M., Ezan, M. A., & Turgut, A. (2018). Thermal performance of a nanofluid-based flat plate solar collector: A transient numerical study. <i>Applied Thermal Engineering</i> , 130, 395–407. https://doi.org/10.1016/j.applthermaleng.2017.10.166 |
| V | Velocity, m/sec | Ghasemi S., Ranjbar A., (2016) Thermal performance analysis of solar parabolic trough collector using nanofluid as working fluid: A CFD modelling study, <i>Journal of Molecular Liquids</i> . 222 159-166. https://doi.org/10.1016/j.molliq.2016.06.091 . |
| W | Aperture of reflector | Gorji, T. B., & Ranjbar, A. A. (2016). A numerical and experimental investigation on the performance of a low-flux direct absorption solar collector (DASC) using graphite , magnetite and silver nanofluids. <i>Solar Energy</i> , 135, 493–505. https://doi.org/10.1016/j.solener.2016.06.023 |
- Greek letters**
- | | |
|---|----------------------------|
| ρ | Density, Kg/m ³ |
| μ | Dynamic viscosity, Pa.sec |
| η | Efficiency |
| Ø | Concentration |
- Subscripts and superscripts**
- | | |
|----|----------------|
| b | Beam radiation |
| f | Fluid |
| fm | Mean fluid |
| i | Inlet |
| np | Nanoparticle |
| nf | Nanofluid |
| o | Outlet |
| ri | Inner receiver |
| r | Receiver |
| th | Thermal |
- Abbreviations**
- | | |
|--------------------------------|-------------------------------|
| Al ₂ O ₃ | Aluminium oxide |
| CNT | Carbon nanotubes |
| CuO | Copper oxide |
| Fe ₂ O ₃ | Hematite |
| HTF | Heat transport fluid |
| INR | Indian rupees |
| LCOE | Levelized cost of energy |
| MWCNT | Multi-walled carbon nanotubes |
| PTC | Parabolic trough collector |
| SiO ₂ | Silicon dioxide |
| SWCNH | Single-walled carbon nanohorn |
| TiO ₂ | Titanium dioxide |
| ZnO | Zinc oxide |
| Fe ₃ O ₄ | Magnetite |
- References**
- Azmi W., Sharma K., Sarma P., Mamat R., Anuar S., Rao V., (2013). Experimental determination of turbulent forced convection heat transfer and friction factor with SiO₂ nanofluid, *Experimental Thermal and Fluid Science* 1–9. <https://doi.org/10.1016/j.expthermflusci.2013.07.006>
- Biswakarma, S., Roy, S., Das, B., & Kumar Debnath, B. (2020). Performance analysis of internally helically v-grooved absorber tubes using nanofluid. *Thermal Science and Engineering Progress*, 18(February), 100538. <https://doi.org/10.1016/j.tsep.2020.100538>
- Bellos E., Tzivanidis C. (2017a). Parametric investigation of nanofluids utilisation in parabolic trough collectors, *Thermal Science and Engineering Progress*, (2017). <https://doi.org/10.1016/j.tsep.2017.05.001>.
- Bellos E. (2018b). A review of concentrating solar thermal collectors with and without nanofluids, *Journal of Thermal Analysis and Calorimetry* <https://doi.org/10.1007/s10973-018-7183-1>.
- Bellos, E., & Tzivanidis, C. (2018c). Thermal analysis of parabolic trough collector operating with mono and hybrid nanofluids. *Sustainable Energy Technologies and Assessments*, 26(August), 105–115. <https://doi.org/10.1016/j.seta.2017.10.005>
- Bobbo, S., Fedele, L., Benetti, A., Colla, L., Fabrizio, M., Pagura, C., & Barison, S. (2012). Viscosity of water based SWCNH and TiO₂ nanofluids. *Experimental Thermal and Fluid Science*, 36, 65–71. <https://doi.org/10.1016/j.expthermflusci.2011.08.004>
- Brinkman H., (1952). The Viscosity of Concentrated Suspensions and Solutions, *Journal of chemical and physics*. 20(4), 571–571. <https://doi.org/10.1063/1.1700493>.
- Coccia G., Di G., Colla L., Fedele L., Scattolini M., (2016). Adoption of nanofluids in low-enthalpy parabolic trough solar collectors : Numerical simulation of the yearly yield, *Energy Conversion and Management*. 118 306–319. <https://doi.org/10.1016/j.enconman.2016.04.013>.
- Comello S., Glenk G., Reichelstein S. (2017). Levelized Cost of Electricity Calculator : A User Guide, *Stanford Graduate School of Business*.
- Dai, Y. ., Huang, H. ., & Wang, R. . (2003). Case study of solar chimney power plants in Northwestern regions of China. *Renewable Energy*, 28(8), 1295–1304. [https://doi.org/10.1016/s0960-1481\(02\)00227-6](https://doi.org/10.1016/s0960-1481(02)00227-6)
- Ebrahimi-bajestan E., Charjouei M., Niazmand H. (2016). Experimental and numerical investigation of nanofluids heat transfer characteristics for application in solar heat exchangers, *International Journal of Heat and Mass Transfer*. 92 1041–1052. <https://doi.org/10.1016/j.ijheatmasstransfer.2015.08.107>.
- Faizal M., Saidur R., Mekhilef S., Potential of size reduction of flat-plate solar collectors when applying MWCNT nanofluid, (2013). *IOP Conference Series: Earth and Environmental Science*. 16 012004. <https://doi.org/10.1088/1755-1315/16/1/012004>.
- Fathabadi H., (2019). Novel solar collector: Evaluating the impact of nanoparticles added to the collector 's working fluid , heat transfer fluid temperature and flow rate, *Renewable Energy*. <https://doi.org/10.1016/j.renene.2019.10.008>.
- Genc, A. M., Ezan, M. A., & Turgut, A. (2018). Thermal performance of a nanofluid-based flat plate solar collector: A transient numerical study. *Applied Thermal Engineering*, 130, 395–407. <https://doi.org/10.1016/j.applthermaleng.2017.10.166>
- Ghasemi S., Ranjbar A., (2016) Thermal performance analysis of solar parabolic trough collector using nanofluid as working fluid: A CFD modelling study, *Journal of Molecular Liquids*. 222 159-166. <https://doi.org/10.1016/j.molliq.2016.06.091>.
- Gorji, T. B., & Ranjbar, A. A. (2016). A numerical and experimental investigation on the performance of a low-flux direct absorption solar collector (DASC) using graphite , magnetite and silver nanofluids. *Solar Energy*, 135, 493–505. <https://doi.org/10.1016/j.solener.2016.06.023>
- Hajabdollahi, H., & Hajabdollahi, Z. (2016). Assessment of nanoparticles in thermoeconomic improvement of shell and tube heat exchanger. *Applied Thermal Engineering*, 106, 827–837. <https://doi.org/10.1016/j.applthermaleng.2016.06.061>
- Hatami, M., & Jing, D. (2017). Optimization of Wavy Direct Absorber Solar Collector (WDASC) using. *Applied Thermal Engineering*. <https://doi.org/10.1016/j.applthermaleng.2017.04.137>
- Hoseinzadeh S., Sahebi S.A.R., Ghasemiasl R., Majidian A. (2017a) Experimental analysis to improving thermosyphon (TPCT) thermal efficiency using nanoparticles/based fluids (water), *The european physical journal plus*, 132 3-10, DOI: 10.1140/epjp/i2017-11455-3
- Hoseinzadeh S., Heyns P., Kariman H., (2019b). Numerical investigation of heat transfer of laminar and turbulent pulsating Al₂O₃/water nanofluid flow, *International Journal of Numerical Methods for Heat and Fluid Flow*. 30 1149-1166. DOI: 10.1108/HFF-06-2019-0485

- Hoseinzadeh S., Heyns P., Taheri S., Khatir M. (2020c). Numerical investigation of thermal pulsating alumina/water nanofluid flow over three different cross-sectional channel, *International Journal of Numerical Methods for Heat and Fluid Flow*. 30 3721-3735. DOI: 10.1108/HFF-09-2019-0671
- Hussein, A. M., Sharma, K. V., Bakar, R. A., & Kadirgama, K. (2013). The effect of nanofluid volume concentration on heat transfer and friction factor inside a horizontal tube. *Journal of Nanomaterials*, 2013. <https://doi.org/10.1155/2013/859563>
- Kalogirou A. (2014) *Solar Energy Engineering Processes and Systems* 2nd edi. Academic press, Oxford
- Kasaiean, A., Sameti, M., Daneshazarian, R., Noori, Z., Adamian, A., & Ming, T. (2018). Heat transfer network for a parabolic trough collector as a heat collecting element using nanofluid. *Renewable Energy*, 123, 439–449. <https://doi.org/10.1016/j.renene.2018.02.062>
- Kaya, H., Arslan, K., & Eltugral, N. (2018). Experimental investigation of thermal performance of an evacuated U-Tube solar collector with ZnO / Etylene glycol-pure water nano fl uids. *Renewable Energy*, 122, 329–338. <https://doi.org/10.1016/j.renene.2018.01.115>
- Kang W., Shin Y., Cho H. (2019). Experimental investigation on the heat transfer performance of evacuated tube solar collector using CuO nanofluid and water, *Journal of Mechanical Science and Technology*, 33 1477–1485. <https://doi.org/10.1007/s12206-019-0249-6>.
- Khin, N., Sint, C., Choudhury, I. A., Masjuki, H. H., & Aoyama, H. (2017). Theoretical analysis to determine the efficiency of a CuO-water nanofluid based-flat plate solar collector for domestic solar water heating system in Myanmar. 155, 608–619. <https://doi.org/10.1016/j.solener.2017.06.055>
- Kim, H., Ham, J., Park, C., & Cho, H. (2016). *Theoretical investigation of the ef fi ciency of a U-tube solar collector using various nano fl uids*. 94, 497–507. <https://doi.org/10.1016/j.energy.2015.11.021>
- Kolekar S., Patil P., (2018). Performance analysis of solar parabolic trough collector system for different concentration of Al₂O₃ with water as base fluid, *International Research Journal of Engineering and Technology*, 5, 2472-2479.
- Krishna Y., Razak R. K. A., Afzal A., (2018). The CFD analysis of flat plate collector- nanofluid as working medium, *AIP Conference Proceedings* 2039-020062 <https://doi.org/10.1063/1.5079021>.
- Kurup, P., Turchi, C. S., Kurup, P., & Turchi, C. S. (2015). *Parabolic Trough Collector Cost Update for the System Advisor Model (SAM)*. November.
- Li Y., Xie H. ,Yu W., Li J., Investigation on heat transfer performances of nanofluids in solar collector, *Materials Science Forum*. 694 (2011) 33–36. <https://doi.org/10.4028/www.scientific.net/MSF.694.33>.
- Ministry of New and Renewable Energy - United Nations Industrial Development Organization (MNRE-UNIDO), (2017). India's CST Sector - Vision 2022.
- Mohammad Zadeh, P., Sokhansefat, T., Kasaiean, A. B., Kowsary, F., & Akbarzadeh, A. (2015). Hybrid optimization algorithm for thermal analysis in a solar parabolic trough collector based on nanofluid. *Energy*, 82, 857–864. <https://doi.org/10.1016/j.energy.2015.01.096>
- Murshed, S. M. S. (2011). Determination of effective specific heat of nanofluids. *Journal of Experimental Nanoscience*, 6(5), 539–546. <https://doi.org/10.1080/17458080.2010.498838>
- Mwesigye A., Huan Z., Meyer J., (2015a) Thermodynamic optimisation of the performance of a parabolic trough receiver using synthetic oil – Al₂O₃ nanofluid, *Applied Energy*. 156 398–412. <https://doi.org/10.1016/j.apenergy.2015.07.035>.
- Mwesigye A., Meyer J., (2017b). Numerical analysis of the thermal and thermodynamic performance of a parabolic trough solar collector using SWCNTs-Therminol®VP-1 nanofluid, *Renewable Energy*, 119 844-862. <https://doi.org/10.1016/j.renene.2017.10.047>
- Nagarajan P., Subramani J., Suyambazhahan S., Sathyamurthy R. (2014) Nanofluids for solar collector applications: A Review, *Energy Procedia*. 61, 2416–2434. <https://doi.org/10.1016/j.egypro.2014.12.017>.
- Nanofluid Price - Platonic nanotech private limited. India. Quotation no- PN/2019-20/1907 (Date- 2/10/2020).
- Ozsoy A., Corumlu V., (2018). Thermal performance of a thermosyphon heat pipe evacuated tube solar collector using silver-water nano fluid for commercial applications, *Renewable Energy*. 122 26–34. <https://doi.org/10.1016/j.renene.2018.01.031>.
- Panchal H., Sadasivuni, K., Muthusamy S., Israr M., Sengottain S. (2021). A concise review on Solar still with Parabolic trough collector. *International Journal of Ambient Energy*. 1-27 DOI: 10.1080/01430750.2021.1922938.
- Phelan P., Otanicar T., Taylor R. (2013) Solar Energy Harvesting Using Nanofluids-Based Concentrating Solar Collector *Journal of Nanotechnology in Engineering and Medicine*, 1–9. <https://doi.org/10.1115/1.4007387>.
- Potenza M., Milanese M., Colangelo G., De Risi A., (2017). Experimental investigation of transparent parabolic trough collector based on gas-phase nanofluid, *Appl. Energy*. 203 560–570. <https://doi.org/10.1016/j.apenergy.2017.06.075>.
- Prof A., Saleh S., (2013). Evaluation of Convective Heat Transfer and Natural Circulation in an Evacuated Tube Solar Collector, *Journal of engineering*, 19 613–628
- Sabiha M., Saidur R., Mekhilef R. (2015) An experimental study on Evacuated tube solar collector using nanofluids, *Transactions on Science and Technology* 2 42–49.
- Sadaghiani, A. K., Yildiz, M., & Koşar, A. (2016). Numerical modeling of convective heat transfer of thermally developing nanofluid flows in a horizontal microtube. *International Journal of Thermal Sciences*, 109, 54–69. <https://doi.org/10.1016/j.ijthermalsci.2016.05.022>
- Shanthi R , Anandan S., Ramalingam V. (2012). Heat transfer enhancement using nanofluids an overview, *Thermal Science* 16(2) 423-444. DOI: 10.2298/TSCI110201003S
- Siavashi, M., Ghasemi, K., Yousofvand, R., & Derakhshan, S. (2018). Computational analysis of SWCNH nanofluid-based direct absorption solar collector with a metal sheet. *Solar Energy*, 170(January), 252–262. <https://doi.org/10.1016/j.solener.2018.05.020>
- Simpson, S., Schelfhout, A., Golden, C., & Vafaei, S. (2018). Nanofluid thermal conductivity and effective parameters. *Applied Sciences (Switzerland)*, 9(1). <https://doi.org/10.3390/app9010087>
- Subramani J., Nagarajan P., Mahian O., Sathyamurthy R., (2017). Efficiency and heat transfer improvements in a parabolic trough solar collector using TiO₂ nanofluids under turbulent flow regime *Renewable Energy*. <https://doi.org/10.1016/j.renene.2017.11.079>.
- Smith, R., Peters, C., & Inomata, H. (2013). Heat transfer and finite-difference methods. In *Supercritical Fluid Science and Technology* (Vol. 4). <https://doi.org/10.1016/B978-0-444-52215-3.00008-8>
- Sundar, L. S., Sharma, K. V, Singh, M. K., & Sousa, A. C. M. (2017a). Hybrid nanofluids preparation, thermal properties, heat transfer and friction factor – A review. *Renewable and Sustainable Energy Reviews*, 68(March 2016), 185–198. <https://doi.org/10.1016/j.rser.2016.09.108>
- Sundar, L. S., Naik, M. T., Sharma, K. V, Singh, M. K., & Siva, T. C. (2012b). Experimental investigation of forced convection heat transfer and friction factor in a tube with Fe 3 O 4 magnetic nanofluid. *Experimental Thermal and Fluid Science*, 37, 65–71. <https://doi.org/10.1016/j.exptthermflusci.2011.10.004>
- Sundar, L. S., Singh, M. K., & Sousa, A. C. M. (2014c). Enhanced heat transfer and friction factor of MWCNT – Fe 3 O 4 / water hybrid nano fl uids ☆. *International*

- Communications in Heat and Mass Transfer*, 52, 73–83. <https://doi.org/10.1016/j.icheatmasstransfer.2014.01.012>
- Taylor R., Pehlan P., Otanicar T., Walker C, Nguyen M., Trimble S., Prasher R. (2011). Applicability of nanofluids in high flux solar collectors, *Journal of Renewable and Sustainable Energy*, 3, 023104 <https://doi.org/10.1063/1.3571565>.
- Tong, Y., Kim, J., & Cho, H. (2015). Effects of thermal performance of enclosed-type evacuated U-tube solar collector with multi-walled carbon nanotube / water nanofluid. *Renewable Energy*, 83, 463–473. <https://doi.org/10.1016/j.renene.2015.04.042>
- Tripathi, P. R., & Bhong, M. G. (2016). *Estimation of Heat Transfer Coefficient and Pressure Drop in a Solar Collector Using Fresnel Lenses*. 5(2), 2014–2017.
- Vajjha R , Das D., (2012) A review and analysis on influence of temperature and concentration of nanofluids on thermophysical properties, heat transfer and pumping power, *International Journal of Heat and Mass Transfer*. 55 4063–4078. <https://doi.org/10.1016/j.ijheatmasstransfer.2012.03.048>.
- Venkata T., Sekhar R., Prakash R., Nandan G., Muthuraman M., (2018). Performance enhancement of a renewable thermal energy collector using metallic oxide nanofluids, *Micro & Nano Letters*, 13-2 248–251, DOI: 10.1049/mnl.2017.0410. doi: 10.1049/mnl.2017.0410
- Waghole D., Shrivastva R. (2014) Experimental Investigations on Heat Transfer and Friction Factor of Silver Nanofluid in Absorber / Receiver of Parabolic Trough Collector with Twisted Tape Inserts, *Energy procedia*, 45 558–567, <https://doi.org/10.1016/j.egypro.2014.01.060>.
- Yu, W., Xie, H., Li, Y., & Chen, L. (2011). Experimental investigation on thermal conductivity and viscosity of aluminum nitride nanofluid. *Particuology*, 9(2), 187–191. <https://doi.org/10.1016/j.partic.2010.05.014>
- Zhang, Z.-X. (2016). Effect of Temperature on Rock Fracture. *Rock Fracture and Blasting*, 111–133. <https://doi.org/10.1016/b978-0-12-802688-5.00005-1>



© 2021. The Authors. This article is an open access article distributed under the terms and conditions of the Creative Commons Attribution-ShareAlike 4.0 (CC BY-SA) International License (<http://creativecommons.org/licenses/by-sa/4.0/>)